ARTICLE

OBC
www.rsc.org/obc

Synthesis and molecular modelling studies of resorcin[4]arene-capped porphyrins † ‡

Bruno Botta,*[a] Paola Ricciardi,[a] Carlo Galeffi,[a] Maurizio Botta,*[b] Andrea Tafi,[b] Rebecca Pogni,[c] Rosa Iacovino,[d] Isidoro Garella,[d] Benedetto Di Blasio[d] and Giuliano Delle Monache*[e]

[a] *Dipartimento di Studi di Chimica e Tecnologia delle Sostanze Biologicamente Attive, Università "La Sapienza", P.le A. Moro 5, 00185 Roma, Italy*

[b] *Dipartimento Farmaco Chimico Tecnologico, Università di Siena, 53100 Siena, Italy*

[c] *Dipartimento di Chimica, Università di Siena, 53100 Siena, Italy*

[d] *Dipartimento di Scienze Ambientali, Seconda Università di Napoli, Caserta, Italy*

[e] *Istituto Chimica del Riconoscimento Molecolare, Università Cattolica del S. Cuore, 00168 Roma, Italy*

Received 3rd April 2003, Accepted 26th June 2003
First published as an Advance Article on the web 21st July 2003

Three new resorcin[4]arene-capped porphyrins (**3**, **5** and **7**) different in the porphyrin skeleton, in the linking arms and in the cavity dimensions, have been synthesised. Molecular modelling calculations explored the conformations and the cavity size of the three compounds and showed that their hydrophobic pockets can accommodate one molecule of water or methane (**3** and **5**), or benzene (**7**) without any distortion. Notably, the capped porphyrin **5** was able to inhibit the oxidation of Co(II) to Co(III), whereas compound **7** did it only partially.

Introduction

Several molecules such as cyclodextrins,[2] crown ethers,[3] cavitands,[4] and calixarenes[5] have been used to build a hydrophobic pocket on top of the metal-containing porphyrin platform to give rise to specific size-shape selectivity in substrate recognition. As a part of our studies on the possible modifications of resorcin[4]arene side chains,[6,7] we focused our attention on the preparation of resorcin[4]arene caps for porphyrins. This paper deals with the building of three resorcin[4]arene capped porphyrins by different synthetic approaches and, as a result, with different cavity sizes shown by molecular modelling calculations and complexations towards Co(II) cations. The three compounds were shown to differ in the complexation of Co(II) cations.

Results and discussion

Synthesis and characterization of resorcin[4]arene capped porphyrins

C-alkylcalix[4]resorcinarenes octamethyl ethers[8] are characterized by high flexibility, but can be converted to a more organised form by reaction at variously functionalised side chains. The tetraalcohol **1a** was treated with commercial coproporphyrin I (**2a**), activated as the acid chloride **2b**, in CH_2Cl_2 at room temperature in the presence of DMAP (Scheme 1). The major product **3** (MH^+ at *m*/*z* 1357 in the FABMS spectrum; Fig. 1 for stereostructure) was isolated from the reaction mixture in 20% yield. The downfield shift of the octamethylene group (δ 60 to 63 in the ^{13}C NMR spectrum) together with the upfield shift of the neighbouring CH_2 (δ 35 to 33) confirmed the acylation of the resorcin[4]arene to have occurred (Table 1). Moreover, the ^1H NMR spectrum of **3** showed in the aromatic region only two singlets, attributable to the protons H_e (that is H-5, H-11, H-17, H-23) and H_i (that is H-25, H-26, H-27, H-28) and in accord with a cone conformation for the resorcin[4]arene moiety, at room temperature.[9] Notably, these signals – as well as those of the side chain – were shifted upfield by the effects of the porphyrin ring current.

Conversely, the porphyrin **4** (synthesised, as a mixture of four non-separable atropoisomers, following the published procedure)[10] and the tetrabromide **1b** (obtained from **1a** with CBr_4 and Ph_3P) were used for the preparation of a second resorcin[4]arene-capped porphyrin with a different chain length (Scheme 2). The condensation of **1b** and **4** in dry DMF with K_2CO_3 at 100 °C gave compound **5** (MH^+ at *m*/*z* 1383 in the FAB MS spectrum; Fig. 2 for stereostructure) in 7% yield. The signal of an oxygenated methylene (at δ 66), substituted in the ^{13}C NMR spectrum of **5** the signal for CH_2Br (at δ 38), while the upfield shift of the aromatic proton signals in the ^1H NMR spectrum of **5** were again evidence of the coupling (Table 2). Only one singlet for both H_e and H_i indicates that the resorcin[4]arene moiety maintained the cone conformation (C_{4v} symmetry).

In the search for a different linking arm and, possibly, better yields, we took into consideration the porphyrin **6a** (Scheme 2), bearing an amino group within the aromatic substituent. The α,α,α,α isomer of **6a**, separable from the three other atropoisomers as a stable crystalline form,[11] was used for the coupling reaction. The resorcin[4]arene **1c**, prepared by alkaline hydrolysis of the ethyl esters in the cone conformation,[8] was treated with **6a** under different reaction conditions [2-chloro-1,3-dimethylimidazolium hexafluorophosphate (CIP)–pyridine–CH_2Cl_2; HOBt–DCC–Et_3N; $(COCl)_2$ and mixed anhydride],[12] but did not afford any isolable product. Therefore, we turned our attention to the activation of the *o*-aminomesophenyl groups of **6a** by reaction with chloroacetyl chloride.[13] The tetrachloroacetamidoporphyrin **6b**, so obtained, gave no coupling product with **1a** either. Only when the amino groups were converted by triphosgene and Et_3N in CH_2Cl_2 at room temperature to isocyanate (**6c**),[14] the nucleophilic attack of **1a** to **6c** (Scheme 2) gave in 10% yield the target compound **7** (MH^+ at *m*/*z* 1555 in the FABMS spectrum; Fig. 3 for stereostructure). The similarity of the spectral data of **7** with those of

† Electronic supplementary information (ESI) available: Benzene-d_6 shifts of compound **7** compared with those of component units, details on the new parameters added to heme29 and cartesian coordinate files of lowest-energy conformations of **3**, **5** and **7** (benzene inside) on the molecular modelling studies (pdb and arc files). See http://www.rsc.org/suppdata/ob/b3/b303741j/

‡ See Ref. 1.

DOI: 10.1039/b303741j

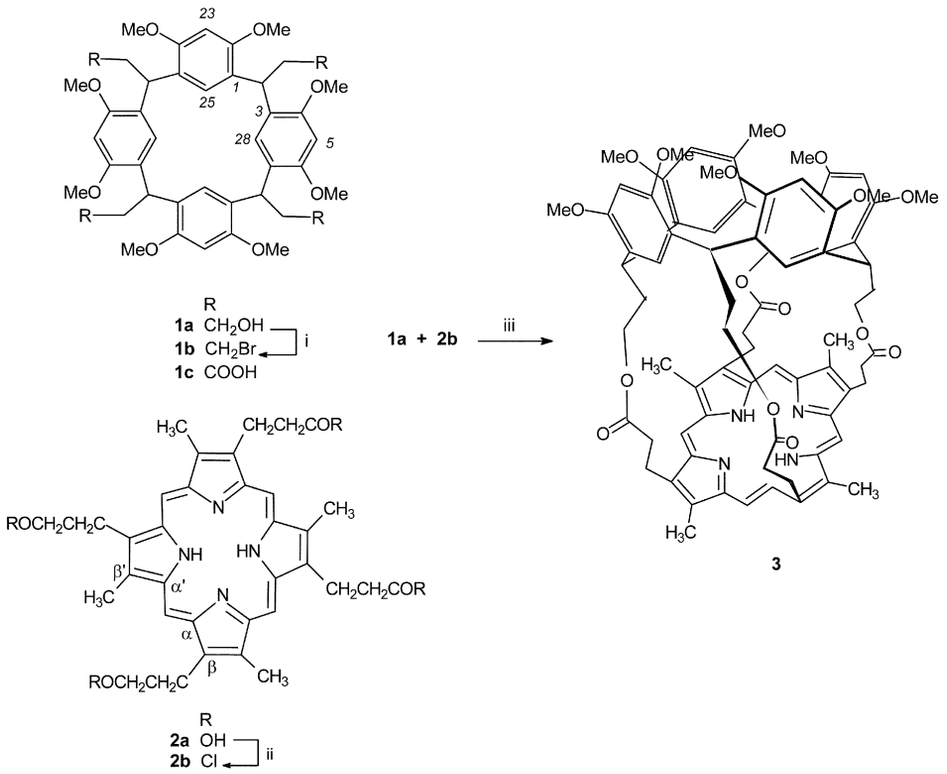

Scheme 1 Synthesis of resorcin[4]arene-capped porphyrin **3**. *Reaction conditions*: i) CBr_4, PPh_3, CH_2Cl_2; ii) $(COCl)_2$, dry DMF, CH_2Cl_2; iii) CH_2Cl_2, DMAP.

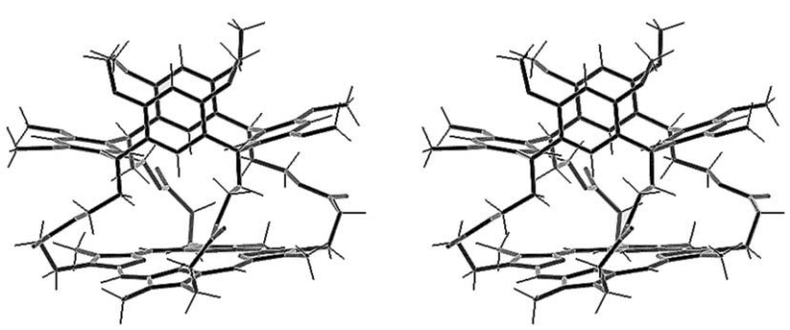

Fig. 1 Three dimensional structures (stereoview) of the lowest energy output conformer of **3**.

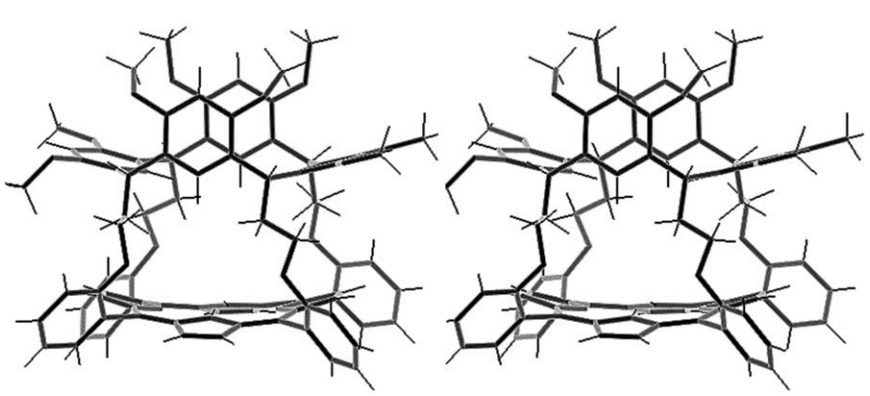

Fig. 2 Three dimensional structures (stereoview) of the lowest energy output conformer of **5**.

the starting compounds **1a** (Table 1) and **6a** (Table 2) argued in favour of the formation of a porphyrin capped by a resorcin[4]arene moiety once again in a cone conformation with the same considerations as above.

Molecular modelling studies

In order to confirm the experimental findings and to evaluate the rigidity of the resorcin[4]arene-capped porphyrins as well as size, shape and chemical features of the intramolecular cavity, computational studies were undertaken.[15] Three types of molecular manipulations were carried out during the simulations: interactive structure building, geometry optimisation and conformational searching. Refined 3D structures, obtained from our previous studies,[8] were utilized as input geometries for the resorcin[4]arenes nucleus. The four arms of each compound connecting the resorcin[4]arene to the porphyrin moiety and the porphyrin itself were manually built

Table 1 ^{13}C- and ^{1}H-NMR spectral data of capped porphyrin (**3**) in comparison with those of the starting resorci[4]arene (**1a**), and the porphyrin methyl ester (**2b**, R = OCH_3)[a]

	3		**1a**		**2b**	
Position	δ_C	δ_H	δ_C	δ_H	δ_C	δ_H
1,3,7,9,13,15,19,21	125.14	—	125.72	—		
2,8,14,20	31.14	4.02 *t* (8,5)	30.94	4.56 *t* (8)		
4,6,10,12,16,18,22,24	155.25	—	155.71	—		
5,11,17,23	97.84	5.92 *s*	96.75	6.33 *s*		
25,26,27,28	125.45	5.52 *br s*	125.45	6.69 *br s*		
OMe	55.77	3.28 *s*	56.02	3.62 *s*		
$-CH_2-$	33.07	1.10 *q* (8)	37.17	2.08 *q* (8)		
$-CH_2O$	63.09	3.57 *t* (7.5)	60.41	3.54 *t* (6.5)		
C=O	172.22	—			173.55	
CH_2 (CO)	37.37	4.65 *ddd* (14,9,3) 4.19 *ddd* (14,10,3)			37.06	4.42 *t* (7.5)
β–CH_2	21.61	3.41 *ddd* (15,10,3) 3.15 *ddd* (15,9,3)			21.94	3.28 *t* (7.5)
β′–CH_3	12.02	3.63 *s*			11.79	3.65 *s*
α	148.58	—			148.65	—
α′	147.44	—			147.52	—
β	137.79	—			138.05	—
β′	137.26	—			136.98	—
meso	96.33	10.03 *s*			96.62	10.02 *s*

[a] $CDCl_3$, 75 and 300 MHz, TMS as internal standard. In the ^{1}H NMR spectrum the signals showed the appropriate integrated intensity. Proton and carbon signals were correlated by HETCOR experiments. Coupling constants (in Hz) are given in parentheses.

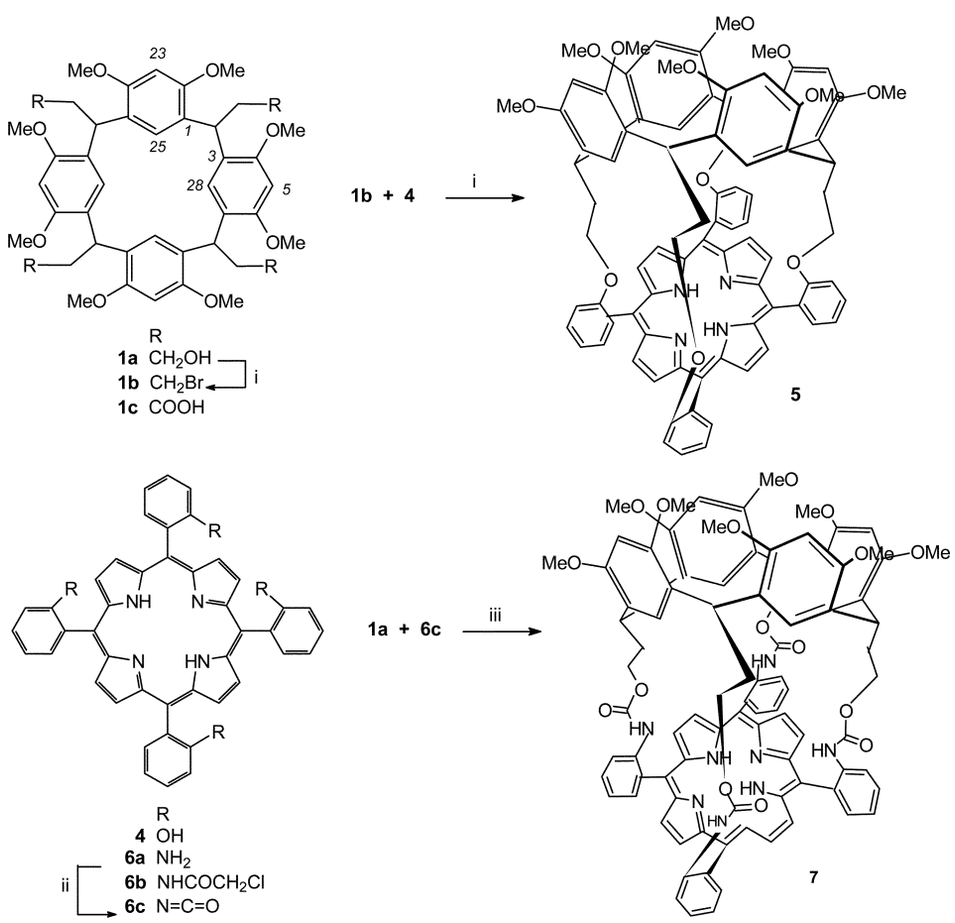

Scheme 2 Synthesis of resorcin[4]arene-capped porphyrin **5** and **7**. *Reaction conditions*: i) dry DMF, K_2CO_3, Argon, 100 °C; ii) triphosgene, Et_3N, CH_2Cl_2; iii) dry CH_2Cl_2, Et_3N, N_2.

using the Fragment Libraries of InsightII. In the absence of parameters suitable to describe capped porphyrins, a preliminary upgrade of the CVFF force field was mandatory. An adapted Heme29 force field[16] was employed and was shown to reproduce bond lengths, bond angles, and even the ruffling of the porphyrin systems. Superimpositions between X-ray structures and the corresponding minimized models gave distance RMS of 0.10 Å for protoporphyrin IX (superimposition of 24 heavy atoms), 0.22 Å for tetraphenylporphyrin (superimposition of 48 heavy atoms) and 0.20 Å for a capped zinc(II) tetraphenylporphyrin (superimposition of 24 heavy atoms of the porphyrin moiety, 24 heavy atoms of the four phenyl rings, the metal ion and the oxygen of the water molecule bound to Zn^{2+}).[17]

Table 2 ^{13}C- and ^{1}H-NMR spectral data of capped porphyrins **5** and **7** in comparison with those of the respective porphyrin (**4** and **6a**)[a]

Position	**5** δ_C	δ_H	**4** δ_C	δ_H	**7** δ_C	δ_H	**6a** δ_C	δ_H
1,3,7,9,13,15,19,21	125.72	—			125.35	—		
2,8,14,20	28.45	3.93 *t* (7.5)			29.38	4.12 *t* (8)		
4,6,10,12,16,18,22,24	155.05	—			155.55	—		
5,11,17,23	95.91	5.93 *s*			95.95	6.01 *s*		
25,26,27,28	124.01	5.21 *br s*			124.52	6.11*s*		
OMe	55.83	3.44 *s*			55.87	3.43 *s*		
$-CH_2-$	35.06	0.32 *br q* (7.5)			35.56	1.34 br *q* (8)		
$-CH_2X$	66.09	3.35 *br t* (7.5)			63.16	3.37 *br t* (8)		
1′	115.73	—	115.85	—	128.89	—	126.78	—
2′	159.60	—	156.00	—	139.14	—	146.69	—
3′	111.46	7.02 *br d* (8)	114.18	7.36 *m*	121.33	7.02 *dd* (8, 1.5)	115.14	6.88 *br d* (8)
4′	129.21	7.67 *td* (8, 1.5)	127.89	7.74 *br t* (8)	130.16	7.44 *br t* (8)	129.61	7.48 *br t* (8)
5′	119.02	7.42 *br t* (7.5)	119.95	7.36 *m*	117.81	7.82 *td* (8, 1.5)	117.50	7.10 *br t* (8)
6′	132.60	8.49 *br d* (7.5, 1.5)	135.47	7.98 *br t* (7)	132.60	8.62 *br d* (8)	134.72	7.79 *dd* (7)
α	133.14	—	130.80	—	133.14	—	129.61	—
β	131.09	8.73 *s*	130.91	8.91 *s*	131.09	8.73 *s*	131.37	
meso	115.08		115.82		115.02		115.82	—
NH	—	12.38 *s*		12.38 *s*		12.30 *s*		12.26 *s*
CONH					152.66	6.06 *s*		

[a] $CDCl_3$, 75 and 300 MHz, TMS as internal standard. In the ^{1}H-NMR spectrum the signals showed the appropriate integrated intensity. Proton and carbon signals were correlated by HETCOR experiments. Coupling constants (in Hz) are given in parentheses

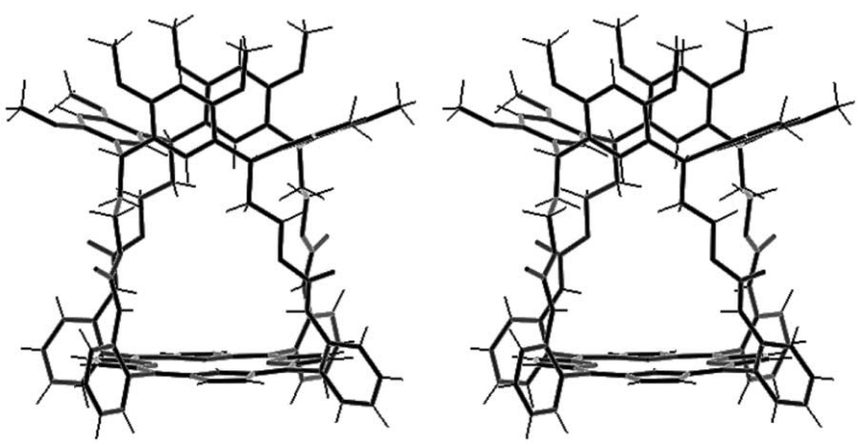

Fig. 3 Three dimensional structures (stereoview) of the lowest energy output conformer of **7**.

The structural complexity of derivatives **3**, **5** and **7** (each one possessing more than 20 rotatable bonds) required the use of molecular dynamics to explore their conformational space. The search was carried out by the discontinuous method of simulated annealing, which had been successfully used for resorcin[4]arenes.[7] The lowest energy output conformations of **3**, **5** and **7** are depicted in Figs 1, 2 and 3, respectively.

In the case of **3** (Fig. 1), all the conformers found in the search (where the steric-energy spanned a range of *ca* 20 kcal mol^{-1}) showed a roughly planar porphyrin moiety and in most of the conformers, the pseudo plane formed by the four methine bridge atoms of the calixarene was nearly parallel to the porphyrin plane. In most of the output conformers (where steric-energy spanned a range of *ca* 15 kcal mol^{-1}) of **5** (Fig. 2) the pseudo plane formed by the four methine bridge atoms was again parallel to the porphyrin plane. By contrast, the porphyrin moiety showed varying degrees of non-planarity.[18] Finally, all the conformers found in the search for **7** (Fig. 3) were distributed in a steric-energy range of *ca* 18 kcal mol^{-1} and the porphyrin moiety appeared to be either planar or tilted in both directions,[18] depending on the spatial orientation of the arms. No correlation was found between the tilting and the steric energy of **7**. Notably, the cone (flattened cone) was the unique geometry of the calixarene cap detected in the conformations of **3**, **5** and **7** populated at room temperature. In order to evaluate and to compare the flexibilities of the collected structures of compounds **3**, **5** and **7**, two dummy atoms – one corresponding to the centroid of the porphyrin ring and the other one corresponding to the centroid of the resorcin[4]arene upper rim – were defined to evaluate the distance between the two building blocks and the degree of twisting of one block with respect to the other. The minimum and maximum distances between the two dummy atoms of **3** were 4.9 Å and 6.6 Å, respectively, while most of the low-energy conformers showed a very small twisting of the calixarene with respect to the porphyrin (*ca* 10°, Fig. 1). In the case of structure **5** (Fig. 2), the minimum and maximum distances between the two dummy atoms were 4.7 Å and 5.6 Å, respectively, while the degree of twisting was quite small as the dihedral angle in almost all the low-energy conformers again showed a value of *ca* 10°. In the case of compound **7** (Fig. 3), however, the distance between the dummy atoms randomly varied without interruption between 7.1 Å and 8.7 Å, the degree of twisting varied approximately from −35° to 35° (without any clear correlation with the steric energy) and, finally, various orientations were found of the pseudo plane formed by the four methine bridge atoms of the calixarene with respect to the porphyrin plane.

In agreement with the above findings and differently from **3** and **5**, compound **7** featured a flexible structure with a repertoire of cavities which could accommodate various shapes of guest molecules.

In order to evaluate in a simple manner the size and chemical characteristics of the intramolecular cavities, complexes of water, methane and benzene with compounds **3**, **5** and **7** were

Table 3 UV-vis spectral data of **3**, **5** and **7**, and their Co-complexes in $CHCl_3$ solution ($c = 1.0 \cdot 10^{-5}$ M, $l = 1$ cm)

Compound	Soret band/nm	Visible region/nm ($\varepsilon/10^4$)
3	408.5	500 (0.55), 537 (0.67), 574 (0.68), 621(0.38)
3-Co(III)	408	540 (2.19), 580 (2.00)
5	422	480 (0.10), 513 (0.12), 553 (0.50), 625 (0.10)
5-Co(II)	424	508 (0.57), 553 (1.23)
7	419	473 (0.60), 512 (0.60), 585 (0.27), 652 (0.18)
7-Co(III)	410	510 (0.59), 542 (1.18)
7-Co(II)	430	

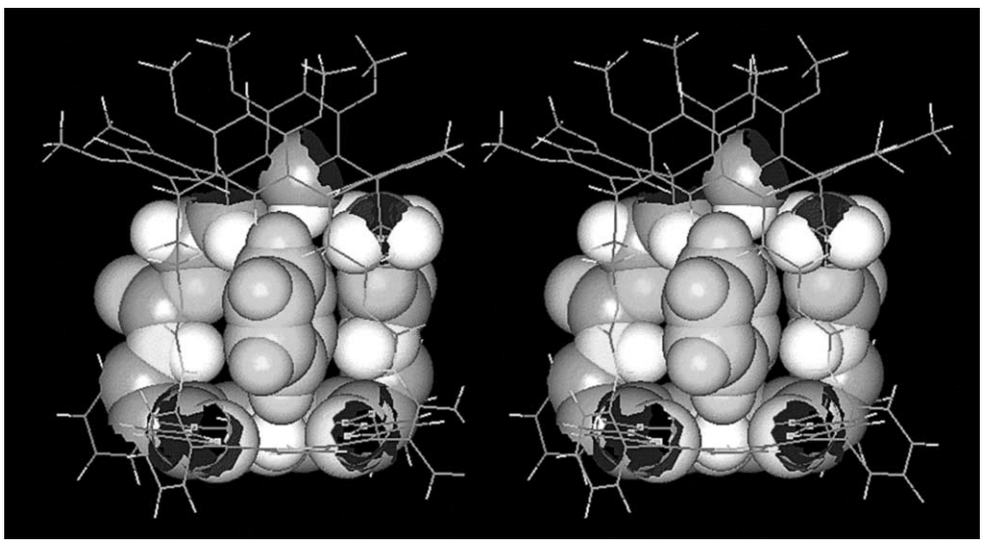

Fig. 4 Three dimensional structure (stereoview) of the complex between **7** and one benzene guest molecule, minimized by molecular modelling.

built and minimized by molecular mechanics. The starting geometries for the complexes were obtained by docking the guest molecules inside the cavity of the lowest energy structure of the three host compounds. The resulting structures were minimized and the output geometry of each complex was compared with the corresponding uncomplexed geometry of the host molecule through atom-by-atom superimposition, in order to verify eventual distortions in the shape of the host caused by the docking. As a result, the capped porphyrins **3** and **5** can accommodate only a water molecule (with a superimposition RMS of 0.04 and 0.05 Å, respectively) or a methane molecule (with RMS of 0.17 and 0.13 Å, respectively). On the contrary, **7** was able to accommodate even a benzene molecule (Fig. 4), without causing any distortion of the minimum-energy conformation of both host and guest compounds (with RMS of 0.13 Å).

To find an experimental support for the results of calculations, *i.e.* to confirm the exclusive interaction between **7** and a molecule of benzene, we ran ^{1}H NMR spectra in C_6D_6 of capped porphyrins and their model moieties and compared the chemical shifts with those in $CDCl_3$. As a result, these experiments revealed that i) **7** is the only capped porphyrin soluble enough in C_6D_6 for an ^{1}H NMR spectrum; ii) the shifts Δ (ppm) = $\delta(C_6D_6) - \delta(CDCl_3)$ of compound **7**, as compared with those of the components, porphyrin **6a** and resorcin-[4]arene **1a** (R = CH_2O–Tosyl), were dramatically different for some of the signals (Table in ESI †). For instance, the signals for H_i and the chain in the resorcinarene were opposite in sign to those of the cap; the same occurred for the H-6′, H-β and NH signals, when the free and the capped porphyrins were compared. The scarcely affected signals all seem to belong to the outside shell of the capped porphyrin, as proof of the insertion of deuterated benzene in **7**.

Complexation experiments

Treatment of **3**, **5** and **7** with Co(II) acetate[19] gave after 72–96 h the metallated compounds **3**-Co (95% yield), **5**-Co (90% yield), and **7**-Co (90% yield). The Soret band in the UV spectrum and two absorption bands (β and α) of similar intensity in the visible region of the spectrum of the **3**-Co complex (Table 3), comparable with those of the porphyrin complexes (**2a**-Co, **4**-Co and **6a**-Co) are characteristic of an octahedral complex, where the oxidized Co(III) cation is hexa-coordinated.[20]

By contrast, the value of the Soret band and the different intensities of α and β bands in the UV-vis spectrum of the **5**-Co complex (Table 3) suggested that the Co(II) cation did not change its oxidation state.[20] Treatment of the **5**-Co complex with $Na_2S_2O_5$, left the UV spectrum unchanged. To confirm these findings, EPR spectra of the **5**-Co(II) complex were run at 77 K and 20 K. At 77 K no result was obtained, whereas at lower temperature an EPR spectrum was detected and attributed to the presence of a high spin **5**-Co(II) complex. The EPR spectrum was characterized by $g_1 = 5.38$, $g_2 = 2.48$ and $g_3 = 1.93$ and no hyperfine structure was resolved.

High spin Co(II) has three unpaired electrons ($S = 3/2$) with a nuclear spin, $I = 7/2$. In every coordination geometry, excited levels are quite close to the ground state, however, so that fast relaxation of the electron spin is occurring.[21] As a consequence the EPR spectra are too broad to be detected at room temperature, and in general the electron spin lattice relaxation time becomes sufficiently long only at temperatures below 30 K. In principle the EPR spectra should be interpreted using an $S = 3/2$ spin Hamiltonian:

$$\hat{H} = \vec{B} \cdot \mathbf{g} \cdot \vec{S} + \vec{S} \cdot \mathbf{D} \cdot \vec{S} + \vec{I} \cdot \mathbf{A} \cdot \vec{S} + \ldots\ldots\ldots$$

where g, D, and A are tensors. The first term refers to the electronic Zeeman interaction, the second is the so called spin–spin interaction which determines the zero field splitting of the electronic energy levels, and the third term is the hyperfine interaction caused by the electron spin-nuclear spin interaction. Other terms, such as nuclear quadrupole effects, are not so important for the interpretation of the electronic structure of the complexes and will be neglected. Spin orbit coupling is

responsible for the zero field splitting of the electronic energy levels.

The splitting of spectroscopic states of high-spin Co(II) in coordination complexes results in two general patterns due to the combined effects of the symmetry of the crystal field and spin orbit coupling. They correspond to a high-spin d^7 configuration either in an orbitally non degenerate ground state ($^4A_2$) or in an orbitally degenerate ground state ($^4T_1$) in which the orbital levels are separated by spin-orbit coupling. In the case of an orbitally non-degenerate ground state, which may be found in tetra- and pentacoordinate sites, the orbital angular momentum is quenched and the combined effects of crystal field symmetry and admixture of excited terms through second-order spin-orbit coupling may lead to a splitting of the two Kramers doublets ($m_S = \pm 1/2, \pm 3/2$) of the $^4A_2$ ground state term in the absence of an applied magnetic field. This is defined as the so-called zero-field splitting as it was shown before in the Hamiltonian. Our EPR data are in favour of a pentacoordination due to the nitrogens of the porphyrin ring and a coordinating molecule from the solvent.[22,23] Furthermore, the UV-vis spectra of pentacoordinated complexes are characterized by the presence of two bands at 16000 cm^{-1} and 18000–22000 cm^{-1}. The spectrum of the **5**-Co(II) complex showed two absorption bands at 18200 cm^{-1} (548 nm) and 16000 cm^{-1} (620 nm), the latter one being considered as diagnostic for a trigonal bipyramidal arrangement.[24]

Finally, the UV-*vis* spectrum of the **7**-Co complex (Table 3) longer wavelength β band had higher intensity than the α band, as typical in Co(II) complexes, whereas in the Soret region two absorption maxima at 410.7 and 430.2 nm were attributed to Co(II) and Co(III) species, respectively.[20] The major wavelength absorption disappeared after bubbling oxygen into the reaction mixture to fulfil the incomplete Co(II) ⟶ Co(III) oxidation. Therefore, it was concluded the complex was a mixture of **7**-Co(II) and **7**-Co(III).

Conclusions

In conclusion, we have synthesized and characterized three different resorcin[4]arene-capped porphyrins (**3**, **5** and **7**). The Heme29 force field, enriched with new parameters, allowed the determination of the dimension of the cavities in the minimized structures of **3**, **5** and **7** by molecular modelling calculations. We are confident that the CVFF force field implemented with these new parameters and calibrated through the correct reproduction of the X-ray structure of known capped-porphyrins,[17] could be extended to other Zn(II)capped-porphyrin systems.

The comparison of the UV-visible spectra of the capped-porphyrin–Co complexes with those of the corresponding porphyrin–Co complexes revealed a different oxidation state for the metal in compounds **5** and (partially) **7**. We conclude that the nature and the length of the linking arms allow modulation of the oxidation of the entrapped Co ion.

Experimental

General remarks

Melting points are uncorrected. ^{1}H and ^{13}C NMR spectra (300 MHz and 75 MHz, TMS = 0 ppm as internal standard in $CDCl_3$ solution). FAB MS (direct inlet).

Resorcin[4]arene octamethylether-capped coproporphyrin I (3)

Oxalyl chloride (0.15 ml, 1.7 mmol) and dry DMF (1 drop) were added to a suspension of coproporphyrin I (**2a**) dihydrochloride (50 mg, 0.07 mol) in dry CH_2Cl_2 (8 ml) under N_2. The mixture was stirred at room temperature in the dark for 1 h. The DMF was then evaporated and the residue was dried under vacuum to eliminate the excess of oxalyl chloride.

The dark purple solid obtained (**2b**) was dissolved in dry CH_2Cl_2 and was added dropwise to a solution of tetra-alcohol **1a** (78 mg, 0.1 mmol) and DMAP (122 mg, 1 mmol) in dry CH_2Cl_2 (20 ml) under N_2. The mixture was left under stirring overnight in the dark at room temperature and the following day was evaporated. Purification by column chromatography ($CHCl_3$–EtOAc, 9 : 1) afforded pure **3** (27 mg, 20%). Compound **3**: vitreous solid; UV-vis ($CHCl_3$) λ_{max}: 241, 283, 402 (Soret), 498, 536, 568, 622 nm. ^{1}H-NMR in Table 1; FAB MS *m*/*z* (int. rel.): 1357 $[MH]^+$ (100), 882 (18), 859 (14), 813 (18), 785 (36).

Tetrabromoresorcinarene (1b)

A solution of PPh_3 (12.4 mmol) in CH_2Cl_2 (8 ml) was added dropwise to a solution of calixarene tetraalcohol (**1a**,[7] 3.5 mmol) and CBr_4 (1.4 mmol) in CH_2Cl_2 (10 ml). The mixture was stirred at room temperature for 20 h and evaporated. Purification by column chromatography (CH_2Cl_2) afforded the tetrabromoresorcinarene **1b** in 58% yield. Mp 263–265 °C; ^{1}H-NMR in Table 2.; EIMS *m*/*z* (int.rel.): 1028 $[M]^+$ (25), 920 $[M - CH_2CH_2Br]^+$(100), 406 $[M - 2 \times CH_2CH_2Br]^{+2}$ (29); m* 823.3 (1028⟶920).

Resorcin[4]arene octamethylether-capped 5,10,15,20-tetra-(*o*-ethoxyphenyl) porphyrin (5)

A solution of bromo calixarene **1b** (350 mg, 0.34 mmol) in dry DMF (14 ml) was added dropwise to a mixture of 5,10,15,20-tetrakis(*o*-hydroxyphenyl) porphyrin **4** (230 mg, 0.34 mmol) and K_2CO_3 (550 mg) in the same solvent (22 ml) at 100 °C under argon. The stirring was continued for another five hours at the same temperature. The reaction was allowed to cool and the DMF was evaporated under vacuum. The residue was taken up in chloroform and the organic layer was washed with water, dried and evaporated to dryness. Column chromatography ($CHCl_3$) afforded the pure capped-porphyrin **5** (32 mg, 7%): vitreous solid; UV-vis ($CHCl_3$) λ_{max}: 422 (Soret), 481, 514, 553, 590, 625 nm. ^{1}H NMR in Table 2; FAB MS *m*/*z* (rel. int.): 1405 $[M + Na]^+$ (50), 1383 $[MH]^+$ (100), 1382 $[M]^+$ (100).

Resorcin[4]arene octamethylether-capped 5,10,15,20-tetra-(o-ethylcarbammophenyl) porphyrin (7)

Triphosgene (120 mg, 0.4 mmol) and Et_3N (255 mg, 2.5 mmol) were added to a solution of α,α,α,α-tetrakis(*o*-amminophenyl)-porphyrin **6a** (200 mg, 0.30 mmol) in dry CH_2Cl_2 (150 ml) under nitrogen. The mixture was stirred at room temperature for 1 h before the addition of a solution of resorcinarene tetralcohol **1a** (200 mg, 0.30 mmol) and Et_3N (146 mg, 1.4 mmol) in dry CH_2Cl_2 (75 ml). The stirring was continued overnight. Evaporation of the solvent and purification by column chromatography ($CHCl_3$) afforded pure **7** (46 mg, 10% yield): vitreous solid; UV vis λ_{max} ($CHCl_3$): 241, 283, 418 (Soret), 512, 542, 584, 652 nm. ^{1}H NMR in Table 2; FAB-MS *m*/*z* (rel.int): 1573 $[M + Na]^+$ (15), 1555 $[MH]^+$ (100), 1554 $[M]^+$ (70).

Co(II) insertion in 3, 5 and 7

To a solution of the resorcinarene-capped porphyrin ($3.6 \cdot 10^{-3}$ mmol) in DMF (2 ml), $Co(OAc)_2$ (0.28 mmol) was added. The mixture was stirred at 45 °C in the dark for 72–96 h, when the UV-vis spectrum revealed the complete insertion of the metal. The solution was concentrated under reduced pressure and the residue was dissolved in $CHCl_3$, washed with water to eliminate the excess of salt and purified by alumina chromatography to give the metallated compounds: **3**-Co (95%), **5**-Co (90%), **7**-Co (90%). UV spectra ($CHCl_3$) are reported in Table 3.

Molecular modelling

All the computational work was carried out on Silicon Graphics workstations (Indigo Entry 4000 and O_2). Molecular

mechanics (MM) and Molecular dynamics (MD) calculations were performed using MSI Inc. softwares (version 95.0) InsightII and Discover.

Few CVFF stretching, bending and torsional parameters were assigned to peculiar bonds of porphyrins **3**, **5** and **7**, which were not directly parametrized in the heme29 force field. The full list of the parameters added or adapted with respect to heme29, together with the atom types used to describe the porphyrin system, is available as Electronic supplementary information †.

The novel torsional parameter implemented to describe the rotation around the bond connecting the porphyrin methine bridges of **5** and **7** to the phenyl rings of the arms was calibrated taking the X-ray structure of a tetraphenylporphyrin as a reference.[17] The torsional barrier around the bond was evaluated through the calculation of an adiabatic torsional potential curve along the dihedral angle, performed with MOPAC-AM1. Both the adiabatic torsional potential curve (energy values) and the implemented parameter are enclosed in the ESI. †

Throughout all calculations a dielectric constant of $\varepsilon = 1.0$ and a scale factor = 0.5 for the 1–4 vdW and the 1–4 electrostatic interactions were used.

Partial atomic charges for MM and MD simulations were obtained through MOPAC calculations, using the MNDO-ESP method. The final charges used for compounds **3**, **5** and **7** are listed in the last column of the three Cartesian Coordinate Files, generated by InsightII and are given in the ESI. † The three files (.arc format) describe the lowest energy conformation of **3** (comp3.arc), **5** (comp5.arc) and **7** (comp7.arc), the last containing also a minimized benzene molecule inside the cavity).

The conformational analysis of **3**, **5** and **7** was performed by the discontinuous method of simulated annealing.[8] To secure a comprehensive sampling of the conformational space, different conformations of the calixarene moiety[9] were used to generate few local minimum-energy geometries of every capped porphyrin, which, in turn, were considered as starting geometries in consecutive simulated annealing runs. Conformational changes of the calixarene macrocycle, in fact, are very low-frequency motions and occur with a very low probability during (single) molecular dynamics runs.[8]

One hundred geometries of each compound were generated at 2 ps intervals through a first 200 ps molecular dynamics sampling performed at 900 K. Each geometry was then minimized with the *Conjugate Gradients* algorithm of molecular mechanics until convergence (average derivative of 0.005 kcal mol^{-1} $Å^{-1}$). A second loop of MD–MM simulations, 2 ps for each conformer previously found followed by a further energy minimization, was performed at 600 K. A third loop of MD–MM simulations was performed at 300 K. The output geometries of the different runs were compared with each other to evaluate the completeness of the search procedure on **3**, **5** and **7**. In all cases the same lowest energy conformation was obtained at least two times from different runs and was reasonably considered as the true global minimum.

The benzene molecule was manually located close to the center of the cavity of the lowest energy conformation of **7**, with the plane of the molecule roughly perpendicular to the plane of the porphyrin. The structure of the system was then refined by energy minimization until convergence (average derivative of 0.001 kcal mol^{-1} $Å^{-1}$).

Acknowledgements

This work was supported by the University "La Sapienza" of Roma, Italy (60% funds) and the University of Siena, Italy (60% funds). We thank Professor J. P. Collman, Stanford University, California, for the useful discussion of the manuscript. This paper is dedicated to Professor Luciano Caglioti and to Professor Domenico Misiti on the occasion of their 70th birthdays.

References and notes

1 Synthesis of *C*-alkylcalix[4]arenes. Part 7.
2 Y. Kuroda, M. Ito, T. Sera and H. Ogoshi, *J. Am. Chem. Soc.*, 1993, **115**, 7003–7004.
3 M. J. Gunter, T. P. Jeynes, M. R. Johnston, P. Turner and Z. Chen, *J. Chem. Soc., Perkin Trans. I*, 1998, 1945–1958.
4 O. Middel, W. Verboom and D. N. Reinhoudt, *J. Org. Chem.*, 2001, **66**, 3998–4005.
5 (*a*) D. M. Rudkevich, W. Verboom and D. N. Reinhoudt, *J. Org. Chem.*, 1995, **60**, 6585–6587; (*b*) D. M. Rudkevich, A. N. Shivanyuk, Z. Brzozka, W. Verboom and D. N. Reinhoudt, *Angew. Chem.*, 1995, **107**, 2300–2302 (*Angew. Chem., Int. Ed. Engl.*, **34**, 2124–2126).
6 B. Botta, G. Delle Monache, M. C. De Rosa, C. Seri, E. Benedetti, R. Iacovino, M. Botta, F. Corelli, V. Masignani, A. Tafi, E. Gacs-Baitz, A. Santini and D. Misiti, *J. Org. Chem.*, 1997, **62**, 1788–1794.
7 B. Botta, G. Delle Monache, G. Zappia, C. Seri, D. Misiti, M. C. Baratto, R. Pogni, E. Gacs-Baitz, M. Botta, F. Corelli, F. Manetti and A. Tafi, *J. Org. Chem.*, 2002, **67**, 1178–1183.
8 B. Botta, M. C. Di Giovanni, G. Delle Monache, M. C. De Rosa, E. Gacs-Baitz, M. Botta, A. Tafi, F. Corelli, A. Santini, E. Benedetti, C. Pedone and D. Misiti, *J. Org. Chem.*, 1994, **59**, 1532–1541.
9 L. Abis, E. Dalcanale, A. Duvosel and S. Spera, *J. Org. Chem.*, 1988, **53**, 5475–5479.
10 M. Momenteau, J. Mispelter, B. Loock and E. Bisagni, *J. Chem Soc., Perkin Trans. 1*, 1983, 189–196.
11 J. P. Collman, R. R. Gagne, C. A. Reed, T. R. Halbert, G. Lang and T. R. Ward, *J. Am. Chem. Soc.*, 1975, **97**, 1427–1433.
12 J. M. Humphrey and A. R. Chamberlin, *Chem. Rev.*, 1997, **97**, 2243–2266.
13 J. P. Collman, B. Boitrl, L. Fu, J. Galanter, A. Straumanis and M. Raptor, *J. Org. Chem.*, 1997, **62**, 2308–2309.
14 J. P. Collman, Z. Wang and A. Straumanis, *J. Org. Chem.*, 1998, **64**, 2424–2425.
15 The MM studies were based on InsightII/Discover (version 95.0; Accelrys Inc., San Diego, USA) software package equipped with CVFF force field.
16 H. D. Hoeltje and C. Fattorusso, *Pharm. Acta Helv.*, 1998, **7**, 271–277.
17 J. P. Collman, P. C. Herrmann, F. Lei, T. A. Eberspacher, M. Eubanks, B. Boitrel, P. Hayoz, Z. Xumu, J. I. Brauman and V. W. Day, *J. Am. Chem. Soc.*, 1997, **119**, 3481–3489.
18 H.-Y. Zhang, A. Blaskò, J.-Q. Yu and T. C. Bruice, *J. Am. Chem. Soc.*, 1992, **114**, 6621–6630 and references cited therein.
19 J. W. Buchler, *Porphyrins*, ed. D. Dolphin, Academy Press, New York, 1979, vol. III.
20 A. Jonson and I. T. Kay, *J. Chem. Soc.*, 1960, 2979–2983.
21 A. Abragam, B. Bleaney, *Electron Paramagnetic Resonance of Transition Ions*, Clarendon Press, Oxford, 1970.
22 L. Banci, A. Bencini, C. Benelli, D. Matteschi and C. Zanchini, *Structure and Bonding*, 1982, **52**, 37–86.
23 M. W. Makinen, L. C. Kuo, M. B. Yim, G. B. Wells, J. M. Fukuyama and J. E. Kim, *J. Am. Chem. Soc.*, 1985, **107**, 5255–5261.
24 M. Ciampolini, *Structure and Bonding*, 1969, **6**, 52–93.